Measurement of internal spatial modes and local propagation properties in optical waveguides

G. H. Vander Rhodes,[a] B. B. Goldberg, and M. S. Ünlü
Departments of Physics and Electrical and Computer Engineering and the Photonics Center, Boston University, Boston, Massachusetts 02215-2421

S. T. Chu, W. Pan, T. Kaneko, and Y. Kokobun
Kanagawa Academy of Science and Technology, Kawaski-shi, Kanagawa 213, Japan

B. E. Little
Research Laboratory of Electronics, Massachusetts Institute of Technology, Cambridge, Massachusetts 02139

(Received 20 May 1999; accepted for publication 20 August 1999)

Internal spatial modes and local properties controlling optical wave propagation have been measured in glass/silica buried waveguides. The period of the observed standing modes provides a direct measure of the local effective index. The measured effective index and transverse modal shape determines the values of all components of the wave vector. In addition, we describe a technique that can obtain detailed information about the locations of remote dielectric interfaces. © *1999 American Institute of Physics.* [S0003-6951(99)05042-1]

Optical guided-wave devices are crucial for routing and control applications in the areas of optical communications and networking. As greater bandwidth requirements have pushed performance demands, guided-wave devices have become increasingly more complex. Increased functionality has been achieved through techniques such as evanescent coupling and resonances in microstructures, effects which strongly depend on local field and propagation properties of the waveguides. While accurate simulations of complicated guided-wave devices rely on assumptions about the physical structure, direct measurement of internal optical modes and the local properties of guided-wave propagation have remained elusive. Using a proximal probe technique, we performed high spatial resolution measurements of evanescent field intensity of guided modes providing detailed quantitative information about the internal modes and their propagation properties.

Near-field scanning optical microscopy[1,2] (NSOM) uses a tapered single mode fiber optic[3] as a subwavelength optical probe. The NSOM probe is sensitive to the local optical fields and, when applied to imaging a surface, samples both evanescent and free-space propagating fields. NSOM studies of waveguides have demonstrated evanescent field decay,[4] standing modes,[5] and recently observed a modulation in the propagation direction[6] due to the Tien effect.[7] To the best of our knowledge, our measurements provide the first observation of standing modes in a single mode waveguide, which allows for the determination of all components of the propagation vector.

The waveguides studied were fabricated using traditional sputtering and optical lithographic methods.[8] They consist of a rectangular compound Ta_2O_5/SiO_2 glass core ($n=1.65$) buried within a SiO_2 cladding ($n=1.44$) region, shown in cross section in Fig. 1(a). Glass waveguides are ideal for an NSOM measurement, due to the relatively large field penetration into air at the sample surface. The experimental arrangement used a lensed fiber to launch light from a tunable external cavity laser into the waveguide under study. Transmitted light at the exit facet is imaged onto both a charge-coupled device (CCD) and photodiode. The NSOM fiber probe is scanned over the top surface of the waveguide, with the collected light routed to an InGaAs photodetector.

The field at the waveguide surface will not be simply related to the internal modes if a large amount of scattering is present. Therefore, a vital initial measurement in this and similar studies is a comparison of the level of scattered light

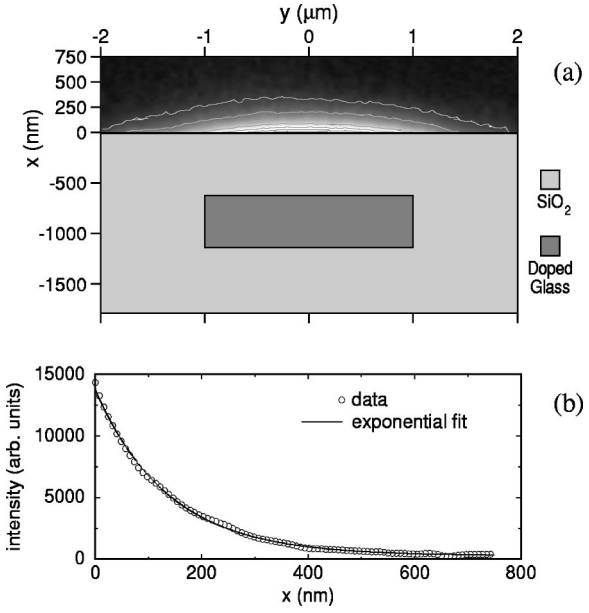

FIG. 1. (a) Measured optical intensity from NSOM scans in the vertical plane, shown on top of a cross section of the waveguides under study. Grayscale map uses black to indicate zero intensity, and white for high intensity. Contours are added to enhance visibility of features. A complete decay of the field at a height *(x)* of around 500 nm is observed. (b) Line cut taken from above at $y=0$, with exponential fit with intensity decay coefficient $(2\alpha_x)=7.34\ \mu m^{-1}$.

[a]Electronic mail: gregvr@bu.edu

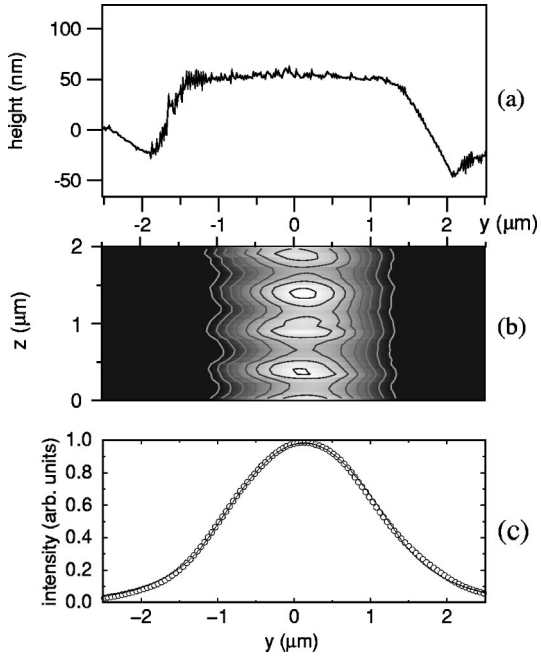

FIG. 2. (a) Line scan of the surface topography across the waveguide, showing ridge at surface due to buried waveguide. (b) Optical image obtained at the surface of the waveguide when TM modes are excited. The periodic variation in the z direction is a standing mode due to a cavity formed in the waveguide. A line cut for $y=0$ exhibits almost pure sinusoidal behavior, with a peak-to-valley ratio of 1.2. (c) Line cut for constant z, with a fit to the lowest order solution in a step-index waveguide.

to that of evanescent field at the surface.[9] The measured optical intensity from NSOM scans in the vertical plane, perpendicular to the direction of light propagation, are plotted in Fig. 1(a) on top of the schematic of the structure. The intensity decays quickly as a function of height showing the absence of scattering into free-space propagating modes. A vertical line cut of this data, shown in Fig. 1(b), exhibits pure exponential behavior consistent with theoretical predictions.

The waveguide studied here is made by first chemically etching a ridge in the core material. Cladding material is then deposited to a thickness matching that of the waveguide core. The cladding above the waveguide core is removed, with the intention of forming a smooth top surface before the deposition of the top cladding layer.[8] However, a slight ridge on the surface above the buried waveguide is observed, shown in Fig. 2(a), allowing us to spatially anchor our optical scans. The actual width of the surface structure does not directly correspond to the buried waveguide dimension since the ridge may not propagate vertically as the top cladding layer is grown.

A large variation with polarization is observed in the NSOM optical scans, because the measured waveguides are not designed for polarization insensitive operation. Shown in Fig. 2(b) is an NSOM image of the TM modes of the waveguide. Selective excitation of only the TM modes is accomplished by controlling the input polarization. The dependence along y of the measured optical intensity is consistent with a single mode waveguide. The periodic variation in the z direction is a standing wave due to the cavity formed between the entrance and exit facets of the waveguide. The period of the standing mode is $\lambda_0/2n_{\text{eff}}$, where λ_0 is the vacuum wavelength, and n_{eff} is the effective index for the

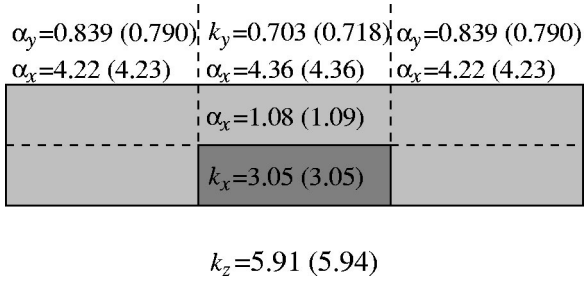

FIG. 3. Measured propagation constants in different regions of the waveguide, all in units of μm^{-1}. Simulated quantities are shown in parentheses.

guided optical mode. At $\lambda_0=1.549$ μm, the measured $n_{\text{eff}}=1.458$ compares very favorably with simulations yielding $n_{\text{eff}}=1.473$. Our scanning stages are interferometrically calibrated, and thus the small discrepancy is, in fact, due to the uncertainty of the waveguide dimensions supplied as input to the simulation.

The component of the wavevector **k** along the propagation direction *(z)* can be obtained directly using the simple relation $k_z=2\pi n_{\text{eff}}/\lambda_0$. The determination of either the x or y component of **k** can then yield the other component through the dispersion relationship: $k_x^2+k_y^2+k_z^2=n^2k_0^2$. In addition, k_y can be obtained from the mode shape across the waveguide. The solutions of a step index waveguide give $\cos k_y y$ (even order) or $\sin k_y y$ (odd order) within the core region, with decaying exponentials outside this region. Figure 2(c) shows a line cut of the NSOM data along the y direction, with a fit to the lowest order solution. The parameters of this fit give k_y and thus k_x in the five regions shown in Fig. 3, with extinction coefficients shown as $\alpha_{x,y}$. The values for k_x and k_y are within 6% of the theoretical predictions shown in parentheses, but the values of α_x are about 20% higher than the values obtained in Fig. 1. We are investigating this decay constant deviation by examining the physical process of evanescent coupling into the NSOM probe as a function of height.

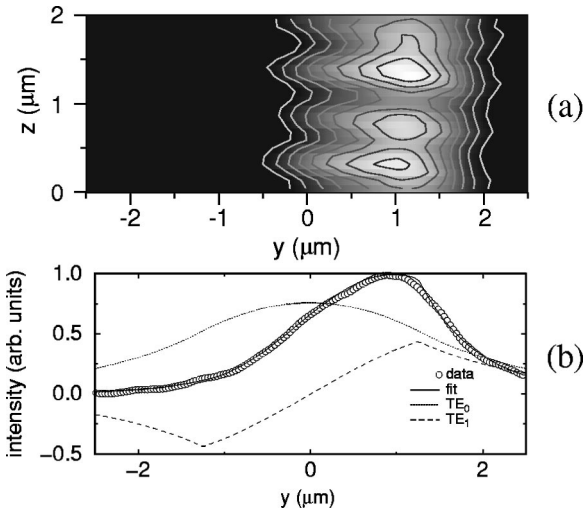

FIG. 4. (a) Optical image obtained at the surface of the waveguide when TE modes are excited. A line cut at $y=1$ μm exhibits mostly sinusoidal behavior, with a peak-to-valley ratio of 1.3. (b) Intensity line cut taken at constant z, with a fit consisting of the weighted superposition of TE_0 (59%) and TE_1 (41%), with a phase difference of 0.098 radians. The theoretical solutions are also shown for TE_0 and TE_1.

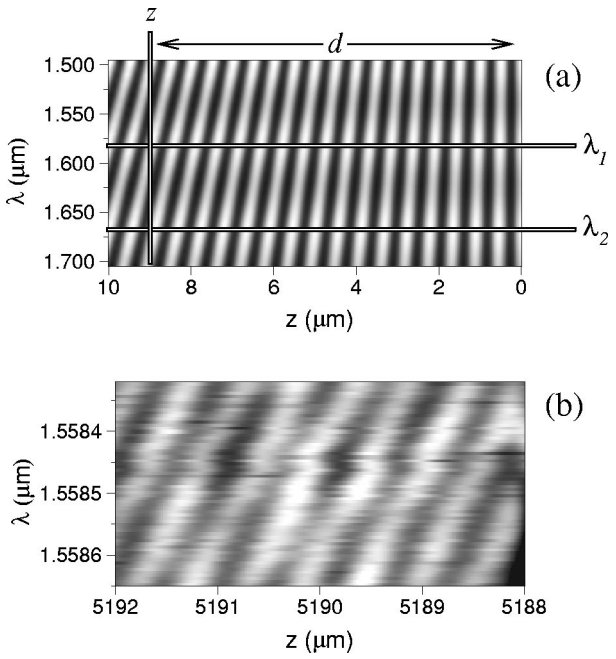

FIG. 5. (a) Simulation of electric field intensity as a function of z and λ for a system with two interfaces, one at $z=0$ μm and one at $z=10$ μm. The propagation direction is in the $-z$ direction. Variables used to identify d are identified. (b) Experimental results for the waveguide. The second interface is again at $z=0$.

For the intended waveguide design, we expect a similar behavior of the guided modes for TE polarization with only minor changes in the mode shapes and **k** values. However, a NSOM scan for TE in Fig. 4(a) is dramatically different: the peak intensity is strongly off-center, indicating a contribution from a higher order mode. The design wavelength is very close to the cutoff condition of the first higher order mode, TE_1. A slight variation in physical parameters could cause the waveguide to become double moded. These two modes have different values for n_{eff}, resulting in an accumulation of phase difference as they propagate, and therefore TE_0 and TE_1 beat against each other. A fit of an intensity line cut taken at constant z, shown in Fig. 4(b), allows us to determine the phase and relative contributions of TE_0 and TE_1.

The entrance and exit facets form a cavity whose length can be determined from the free spectral range (FSR) in the transmission spectrum. As expected, the measured FSR (0.19 nm in wavelength) corresponds to a cavity formed between the input and output facets (separated by 9 mm). While the transmission measurements can provide information about the overall cavity length, the absolute position of a dielectric interface (or possibly a defect) along the waveguide cannot be determined. We have developed a simple and direct measurement which allows for identifying the precise location of any local or remote interfaces. Figure 5(a) shows schematically the standing waves formed in the presence of dielectric interfaces as a function of wavelength. The wavelength (λ) dependence of the intensity at a constant z provides information about the distance d of this measurement point (the tip location) to the output interface given by $d=\pi\lambda_1\lambda_2/2(\lambda_1-\lambda_2)$, where λ_1 and λ_2 are defined in Fig. 5(a).

To test the accuracy of this technique, we measure the standing mode in the waveguide as a function of wavelength in Fig. 5(b). Using the above analysis, we obtain a distance d of 5.19 mm, matching the distance from the probed region to the exit facet. This is an obvious result, but it should be understood that for more complex devices, which switch outputs or have complicated resonances, this technique could give a wealth of information about the various dielectric interfaces.[10]

In conclusion, we have demonstrated the determination of all components of the wavevector from detailed proximity probe measurement of the standing modes and spatial distributions in a single mode waveguide. More complex waveguide devices, including ring resonators,[8] are currently under study.

We thank the support of the National Science Foundation (ECS-9625236, DMR-9413855, and DMR-9701958) as well as the Department of Education under Grant No. P200A50267-97.

[1] U. Durig, D. W. Pohl, and F. Rohner, J. Appl. Phys. **59**, 3318 (1986).
[2] B. B. Goldberg, M. S. Ünlü, W. D. Herzog, and E. Towe, IEEE J. Sel. Top. Quantum Electron. **1**, 1073 (1995).
[3] E. Betzig, J. K. Trautman, T. D. Harris, J. S. Weiner, and R. L. Kostelak, Science **251**, 1468 (1991).
[4] D. P. Tsai, H. E. Jackson, R. C. Reddick, S. H. Sharp, and R. J. Warmack, Appl. Phys. Lett. **56**, 1515 (1990).
[5] P. L. Phillips, J. C. Knight, B. J. Mangan, P. S. J. Russell, M. D. B. Charlton, and G. J. Parker, J. Appl. Phys. **85**, 6337 (1999).
[6] S. Bourzeix, J. M. Moison, F. Mignard, F. Barthe, A. C. Boccara, C. Licoppe, B. Mersali, M. Allovon, and A. Bruno, Appl. Phys. Lett. **73**, 1035 (1998).
[7] P. K. Tien, J. P. Gordon, and R. Whinnery, Proc. IEEE **53**, 129 (1965).
[8] B. E. Little, S. T. Chu, W. Pan, D. Ripin, T. Kaneko, Y. Kokubun, and E. Ippen, IEEE Photonics Technol. Lett. **11**, 215 (1999).
[9] G. H. Vander Rhodes, M. S. Ünlü, B. B. Goldberg, J. M. Pomeroy, and T. F. Krauss, IEE Proc. Optoelectron. **37**, 379 (1998).
[10] G. H. Vander Rhodes, B. B. Goldberg, M. S. Ünlü, S. T. Chu, and B. E. Little (unpublished).